

01 May 1987

University of Missouri–Rolla Cloud Simulation Facility: Proto II Chamber

Daniel R. White

Missouri University of Science and Technology

James L. Kassner

Missouri University of Science and Technology

John C. Carstens

Missouri University of Science and Technology, carstens@mst.edu

Donald E. Hagen

Missouri University of Science and Technology, hagen@mst.edu

et. al. For a complete list of authors, see https://scholarsmine.mst.edu/phys_facwork/737

Follow this and additional works at: https://scholarsmine.mst.edu/phys_facwork



Part of the [Aerospace Engineering Commons](#), [Chemistry Commons](#), and the [Physics Commons](#)

Recommended Citation

D. R. White and J. L. Kassner and J. C. Carstens and D. E. Hagen and J. L. Schmitt and D. J. Alofs and A. R. Hopkins and M. B. Trueblood and M. W. Alcorn and W. L. Walker, "University of Missouri–Rolla Cloud Simulation Facility: Proto II Chamber," *Review of Scientific Instruments*, vol. 58, no. 5, pp. 826-834, American Institute of Physics (AIP), May 1987.

The definitive version is available at <https://doi.org/10.1063/1.1139640>

This Article - Journal is brought to you for free and open access by Scholars' Mine. It has been accepted for inclusion in Physics Faculty Research & Creative Works by an authorized administrator of Scholars' Mine. This work is protected by U. S. Copyright Law. Unauthorized use including reproduction for redistribution requires the permission of the copyright holder. For more information, please contact scholarsmine@mst.edu.

University of Missouri–Rolla cloud simulation facility: Proto II chamber

Daniel R. White

Department of Engineering Mechanics and Graduate Center for Cloud Physics Research, University of Missouri–Rolla, Rolla, Missouri 65401

James L. Kassner

Dexter D. Hulsart Company, Inc., P. O. Box 1878, Tuscaloosa, Alabama 35401

John C. Carstens, Donald E. Hagen, and John L. Schmitt

Department of Physics and Graduate Center for Cloud Physics Research, University of Missouri–Rolla, Rolla, Missouri 65401

Darryl J. Alofs

Department of Mechanical Engineering and Graduate Center for Cloud Physics Research, University of Missouri–Rolla, Rolla, Missouri 65401

Alfred R. Hopkins, Max B. Trueblood, and Max W. Alcorn

Graduate Center for Cloud Physics Research, University of Missouri–Rolla, Rolla, Missouri 65401

William L. Walker

Kel-tec Corp., 84 Hill Avenue, Fort Walton Beach, Florida 32548

(Received 3 July 1986; accepted for publication 13 January 1987)

The Graduate Center for Cloud Physics Research at UMR has developed a cloud simulation facility to study phenomena occurring in terrestrial clouds and fogs. The facility consists of a pair of precision cooled-wall expansion chambers along with extensive supporting equipment. The smaller of these chambers, described in this article, is fully operational, and is capable of simulating a broad range of in-cloud thermodynamic conditions. It is currently being used to study water drop growth and evaporation for drops nucleated (activated) on well-characterized aerosol particles. Measurements have been made not only for continuous expansions (simulated updraft) but also for cyclic conditions, i.e., sequences of expansion-compression cycles resulting in alternating drop growth and evaporation. The larger of the two cloud chambers is nearing completion and will provide a broader range of conditions than the smaller chamber. The facility is supported by a fully implemented aerosol laboratory which routinely produces well-characterized condensation nuclei. The aerosol laboratory contains extensive instrumentation designed to both shape and measure the size distribution and nucleating characteristics of the generated aerosol. The cloud simulation facility also includes a humidifier to bring an air sample to a known humidity before it is put into the cloud chamber. A systematic program to infer effective condensation coefficients (of water vapor on cloud drop) under a variety of well-controlled simulated in-cloud conditions is now under way. Analysis of current experiments with standard drop growth theory indicates a variation of condensation coefficient with observation time, with values sufficiently low to explain one of the current mysteries in cloud physics: *viz.*, the broad spread of drop sizes observed in natural clouds. This article includes a description and performance specifications of the smaller cloud simulation chamber.

INTRODUCTION

During the past 25 years the Graduate Center for Cloud Physics Research at the University of Missouri–Rolla has been engaged in a balanced theoretical and experimental study of the microphysical processes active in atmospheric clouds and fogs. In 1968 a program was initiated to develop a laboratory facility for simulating cloud thermodynamic processes. Two cooled-wall expansion cloud chambers are the heart of the resulting UMR cloud simulation facility. The

two chambers, designated Proto II and Romulus, are designed to subject a sample of moist aerosol-laden air to a predetermined profile of temperature and pressure approximating those observed during various processes which occur in the atmosphere. This article describes the smaller Proto II chamber. A summary of the chamber operating parameters is given in Table I.

Cooling the walls at the same rate as the gas in the chamber greatly reduces the exchange of heat between the sample and the chamber walls, thereby minimizing thermal

TABLE I. Proto II chamber operating parameters.

Temperature Range:	40 to -40 °C
Control:	
Holding:	At fixed temperature rms deviation from spatial average, 40 sensors
Cooling:	Maximum rate
	Wall temperature lag from control point rms deviation from spatial average
Temperature measurement resolution	0.030 °C
Temperature measurement accuracy	10 °C//min
Pressure	0.01 °C/(°C/min) ^a
Reference pressure absolute accuracy:	± 0.01%, dead weight pressure gauge
Dynamic sensor range:	0-15 kPa differential
Resolution:	± 0.006 kPa
Control:	
Holding:	Standard deviation with time about average
Expansion:	Maximum rate
Offset from command	0.065 kPa
Standard deviation with time	0.5 kPa/s (12 °C/min wet adiabatic)
Wall cooling method	0.065 kPa
	0.05 kPa
	Thermoelectric modules plus fluid thermostating of heat sinks
Sensitive volume dimensions	
Diameter:	46 cm
Height:	
One section:	61 cm
Two sections:	122 cm

^a Cooling rate.

uncertainties. The facility thus provides an opportunity to observe and study various atmospheric processes under prolonged, controlled, measurable, and repeatable conditions. No comparable facility exists elsewhere, nor to our knowledge is one being planned elsewhere.

An extensive array of support equipment has also been developed. This includes several types of aerosol generators for producing both water soluble and insoluble particles; as well as equipment to modify and characterize the generated aerosol based on both size and ability to nucleate water drops or ice crystals. Measurements can be made on cloud droplets formed in the chambers both *in situ* and by extraction of the sample from within the chamber. Figure 1 shows a flow diagram for the facility with arrows tracing the progress of an aerosol sample flowing through the system. The details of the support equipment either have been¹⁻³ or will be reported elsewhere.

The philosophy behind this facility embraces the recognition that the development of a cloud is governed by a combination of microphysical and dynamic processes. The simulation facility is intended to investigate the microphysical processes with the conviction that both types of processes

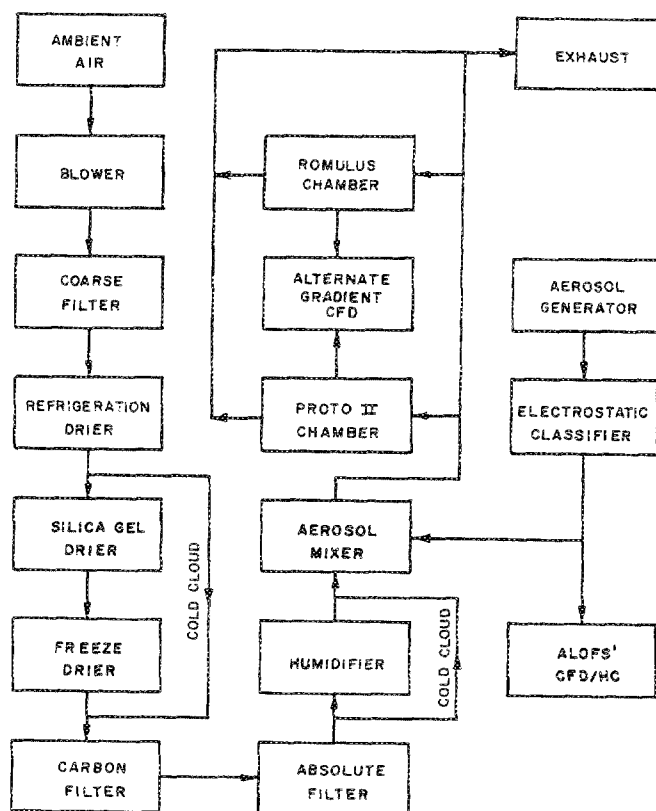


FIG. 1. Flow diagram of UMR simulation facility.

must be understood individually before there is any realistic hope of a clear understanding of their combined interactive effects on the cloud.

Some areas of study under current or proposed investigation include: warm and cold cloud droplet growth, aerosol scavenging by cloud droplets, ice nucleation and growth, collision coalescence, memory effects due to cycles of condensation and evaporation, and optical properties of clouds.

I. PROTO II CHAMBER

A. Physical description

The Proto II chamber is a cooled-wall expansion cloud chamber. The chamber is a 10-sided vertical cylinder with a flat to flat internal dimension of approximately 46 cm (Fig. 2). It is designed to be operated with internal heights of 61 or 122 cm. Initial experiments have been done in the 61-cm configuration.

The design concept for this chamber is to provide the interior wall surfaces with a means of external temperature control so that a temperature match between the walls and gas is maintained as the gas temperature is changed by expansion or compression. In this way the massive flux of heat to or from the walls found in an expansion cloud chamber⁴ is avoided, and the interior temperature remains well defined. The chamber can be programmed to carry out expansions at any rate slower than the maximum design rate, stop and hold constant temperature and pressure, reverse and recompress, or any combination of these while maintaining accurate

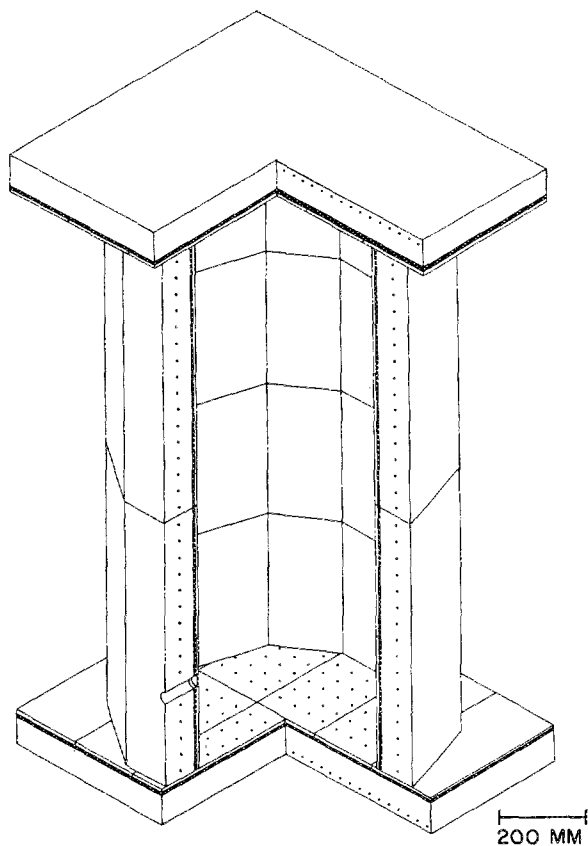


FIG. 2. Proto II chamber.

knowledge of the thermodynamic parameters of the sample.

The chamber can operate with interior wall temperatures between $+40$ and -40 °C. Considerable care has been taken to ensure uniform interior wall temperature. Temperature control is based on the use of thermoelectric modules (TEM's) to pump heat between the thin (0.96 cm) inner wall and the thick (7.6 cm) fluid-thermostated outer wall. Figure 3 shows a cross section of the chamber wall. It should be noted that the inner wall plates are actually two aluminum plates (6.35 and 3.18 mm) laminated together with a heat-cured sheet adhesive. In addition to permitting the use of inserts for the sockets into which the mounting studs screw, the reduced thermal conductivity in the adhesive bond line causes an increased thermal resistance for transfer of heat from the inner chamber surface to the TEM interface. This results in a significant smoothing of the temperature over the inner chamber surface compared to that observed when single solid plates of equal total thickness were tested. The beveling of the plate edges is done because otherwise the row of TEM's near the plate edge would be cooling a greater mass than the other TEM's, resulting in a slower response at the plate edge than the center.

TEM's were chosen because they can provide a more spatially uniform temperature than would be possible, for example, by circulating a liquid through passageways in the walls of the chamber. Moreover, the heat pumping of the TEM's can be precisely controlled by direct electrical

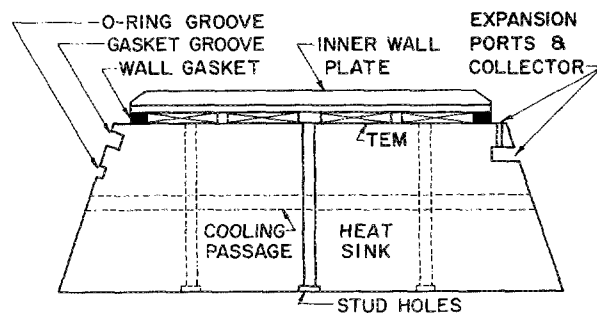


FIG. 3. Cross section of chamber wall.

means. The area controlled by a single control loop has been kept small (15.25×30.5 cm) with each control loop (40 for the 61 cm height; 60 for the 122 cm height) having its own interior wall temperature sensor, analog control circuit, programmable switching power supply, and set of TEM's. In this chamber each interior wall plate has one control loop.

The TEM's can cool the inner wall surface at rates up to 10 °C/min for temperatures from $+40$ to 10 °C below the temperature of the heat sink. Below this range the maximum cooling rate decreases until the lowest temperature of 35 °C below the heat sink temperature is reached. Maximum heating rate exceeds 10 °C/min for all temperatures. At present the chamber at 20 °C regularly shows an rms spread of 0.01 °C or less in the temperature of the 40 measured control sections with a peak-to-peak spread of less than 0.050 °C. For the interior walls 30 °C below the heat sink temperature, the rms increases to 0.075 °C and the peak-to-peak spread approaches 0.5 °C.

B. Temperature measurement

Temperatures are measured using transistor thermometers developed and constructed by the electrical engineering staff of this research center. The thermometers use the temperature characteristics of the base-to-emitter junction of a transistor as the sensor. Their useful range of ± 50 °C covers the temperature range of interest for work with the simulation facility.

The system is calibrated to an output of 0.000 V dc at 0.0 °C and a gain of -0.100 V dc/°C. The slight quadratic nonlinearity (0.07 °C maximum error) is compensated for by computer corrections when the thermometers are read. The system has a resolution of ± 0.001 °C and can be calibrated to ± 0.005 °C. Long-term zero point drift for 6–12 months is typically less than ± 0.010 °C.

Thermometer calibration is based on a water triple point cell and National Bureau of Standards gallium melting point cell. A commercial electronic quartz thermometer and a commercial direct reading platinum resistance thermometer are used as transfer and interpolation standards.

The chamber wall plate and heat sink transistor sensors are mounted in a threaded brass rod (1.3 cm long and 0.5 cm in diameter) which can be screwed directly into flat bottom-

tapped threaded wells in either the interior wall plate (Fig. 4) or the heat sink. The sensor threads are coated with a small amount of thermal grease which assures maximum thermal contact between the sensor and the part being measured. One sensor is located in the center of each interior wall plate and there is one heat sink sensor for every two interior wall plates.

The facility has 128 thermometers of which 96 can be read directly by the primary control and data-acquisition computer (NOVA 840; Data General Corp.) at a rate of 40 Hz. Sixty of these 96 channels are assigned to the chamber inner wall plate thermometers and 14 to chamber heat sink thermometers. The remaining 22 channels are assigned to thermometers distributed throughout the rest of the facility in such locations as the sample humidification system, various fluid coolant loops, etc.

C. Temperature control

The interior surface temperature of the chamber wall is controlled by separate analog controller circuits for each 15.25×30.5 -cm control section of the wall. The controllers are proportional with both integrator and differentiator components. Each controller has two inputs, one from the output of the thermometer mounted in the wall section and the second from the D/A (digital-to-analog) channel of the NOVA 840 control computer (see Sec. II A), which is proportional to the desired wall temperature. The controller generates an error signal by comparing the two signals and, after modifying the error signal with the integrator and differentiator contributions, outputs the result as a command signal to the appropriate programmable switching power supply which then causes the wall section to heat or cool as necessary to drive the error signal to zero. This closed-loop system has a settling time of approximately 30 s.

The desired temperature signal is provided by the control computer as a function of time through a dedicated D/A channel which is updated every 0.5 s. The desired temperature is calculated by linear interpolation between points stored in a computer file. The particular file consisting of 1001 time-temperature-pressure sets is entered as part of the chamber closing sequence after the initial conditions and actual sample characteristics are known, and the appropriate file can be selected from the available control file library.

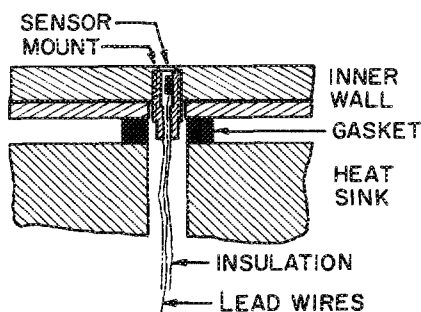


FIG. 4. Mounting of thermometers in chamber inner wall.

The thermal mass of the inner wall plate introduces a natural delay into the response of the chamber to changes in dT/dt , where T is the temperature. This appears as a lag when the rate is increased and an overshoot when the rate is reduced. However, the response of the chamber is sufficiently repeatable that temperature data collected during previous expansions can be used to modify the control signal to the controllers to provide the required anticipation which minimizes both lags and overshoots.

Even the uncorrected response of the chamber for a typical $10^\circ\text{C}/\text{min}$ linear cooling profile shows a maximum initial error between the measured and desired temperatures of less than 0.8°C . This decreases to between 0.15 and 0.18°C within 15 s after the beginning of the cooling and remains relatively constant during the period of linear temperature decrease. At the end of the cooling period there is an overshoot of approximately 0.5°C with recovery in less than 10 s.

The temperature of the chamber heat sink is controlled by circulating fluid from a constant temperature bath (Forma Scientific, Model 2075A) through passages drilled in the heat sinks expressly for this purpose (Fig. 3). The flow pattern in the chamber heat sink consists of opposing flows in adjacent passages. This ensures a more uniform temperature distribution by averaging the effects of the increase in fluid temperature between inlet and outlet ports. Response of the heat sink and circulator bath to changes in desired temperature is sufficiently slow to preclude effective changes during the course of most individual experiments.

D. Pressure measurement

Pressure is measured in the chamber by a differential strain gauge pressure transducer with its reference side connected to the sensing volume of a vacuum-referenced precision (0.01%) dead weight gauge (Ruska, Model 2465, 0–103 kPa). The pressure sensor is located external to the chamber and connected to the sensitive volume of the chamber by a 3.17-mm-i.d. tube and a hole drilled through the chamber wall. The response of the transducer and connecting tube is much faster than any rates of pressure changes within the design range of the chamber. This arrangement simplifies the exchange of transducers so that the range of the transducer can be matched to the anticipated peak-to-peak pressure change during a particular experiment. Therefore, the sensitivity of the system can be maximized for each type of experiment. The reference pressure can also be varied to center the transducer range on the anticipated absolute pressure range of the chamber. The pressure port is located in one of the lower side wall sections of the chamber.

Calibration of the differential pressure transducers is performed using two of the precision dead weight pressure gauges to apply accurately known pressures to each side of the transducer. At each setting (when both gauge pistons are floating) the difference in the settings is entered into the computer and the output signal of the transducer recorded by the computer through the same A/D (analog-to-digital) system used for experimental readings. Once the full range of calibration readings has been recorded, a least-squares cubic

curve is fit to the data. Calibration data are taken for pressure changes in both directions.

During operation, one of the dead weight gauges is covered by a bell jar with a vacuum pump connected to the volume above the piston. The reference side of the transducer is connected to the bottom side of the piston and a precision fine metering valve is used to bleed filtered air into the transducer reference lines. The metering valve is adjusted so that the amount of bleed air entering the system just balances that which is lost by flow past the piston to the vacuum in the bell jar. In this way a steady-state condition with the piston floating can be maintained for periods of time in excess of those required to carry out an experiment.

The accuracy of the system is three parts in 10^4 . The effects of electrical noise in the system are reduced by reading the pressure transducer signal 50 times at a 10-kHz rate with the high-level A/D unit of the control computer (NOVA 840) and averaging the readings.

E. Pressure control

The cloud chamber pressure versus time control profile is designed to cause the gas temperature to track the chamber wall temperature (see Sec. I B). Pressure control is maintained by removing or adding air to the chamber by means of isentropic expansions or compressions. While the amount of air added during compression is restricted to very small volumes the amount removed during expansions can be quite large. The rate of air flow into or out of the system is controlled by an 8-bit digital valve (Digital Dynamics, Inc.). This valve has eight parallel orifices which are individually controlled and have their individual flow rates arranged in a binary sequence. That is, if the orifices are numbered $n = 0, 1, 2, \dots, 7$, the relative flow through a given orifice for a given set of inlet and outlet pressures is proportional to 2^n . Each bit of the valve is controlled by the corresponding bit of an 8-bit digital word from the NOVA 840 control computer.

During operation the chamber pressure is measured, the desired chamber pressure one update period in the future (normally 1 s) is determined from the preloaded time-temperature-pressure control profile, and the required valve setting is calculated based on pressures and required pressure changes. The valve setting is converted to an 8-bit digit word and sent to the digital output controlling the valve. A major advantage of this system is the speed of valve response since the valve setting can be changed from fully closed to fully open, or anything in between, in a single jump. This reduces the peak-to-peak oscillations in pressure, associated with the control system, by a factor of 50 compared to a former motor-driven rotary valve system. The sign of the calculated pressure change determines whether the expansion or re-compression system is used.

F. Expansion system

The expansion system of the chamber removes air radially from the sensitive volume through a series of small ports (16 0.79-mm-diam holes per 61 cm of height) located along

each of the ten vertical joints between side wall heat sink sections (Fig. 5). The individual flows are combined and directed to the expansion manifold located under the chamber. The design provides balanced flow in all the lines so that air can be removed or introduced into the chamber uniformly at all ten joints.

G. Optical systems

A schematic view of the optical system for the chamber is shown in Fig. 6.

1. Chamber windows

The optical cloud diagnostic techniques outlined below access the chamber via 2.3-cm (clear aperture) windows. The chamber has three windows: two directly opposite each other and one at 72° from the forward direction.

All window assemblies are of the same design (Fig. 7). Each has a 1.6-mm-thick sapphire window, mounted in Delrin with an O-ring seal to the inner wall, which is approximately coplanar with the inner surface. Sapphire was selected because it is very tough and has an unusually high thermal conductivity for a transparent material. The sapphire windows are flat to one wavelength, have been cut for minimum birefringence, and are coated. About 4 mm behind the sapphire wall window provisions are made to mount another optical element. This can be a prism, lens, or another sapphire window. The entire system is mounted in a Delrin cylinder that is easily removed without disassembly of any other part of the chamber.

The temperature of the window can be controlled to track the walls. This is accomplished by allowing thermostated carbon dioxide gas to flow between the inner and wall plate windows; the gas temperature determines the temperature of the wall window. A transistor thermometer sensor is in contact with the edge of the wall window and its signal is used for control. Very cold carbon dioxide gas is generated by the phase change from liquid to gas in the compressed gas cylinder and a subsequent nozzle expansion. The gas is then heated by a controlled electrical resistance heater to the required temperature and allowed to flow through the space between the windows.

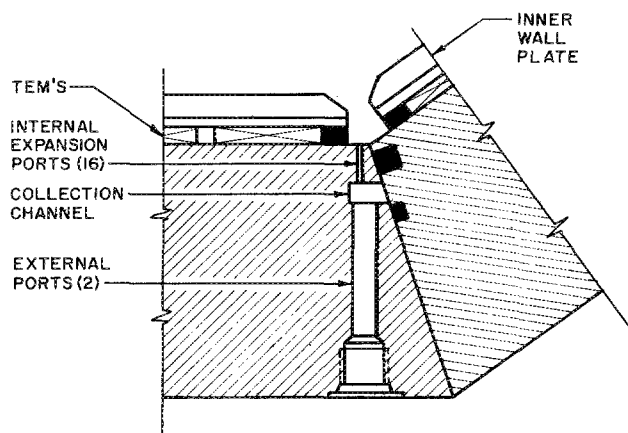


FIG. 5. Expansion manifold in chamber wall.

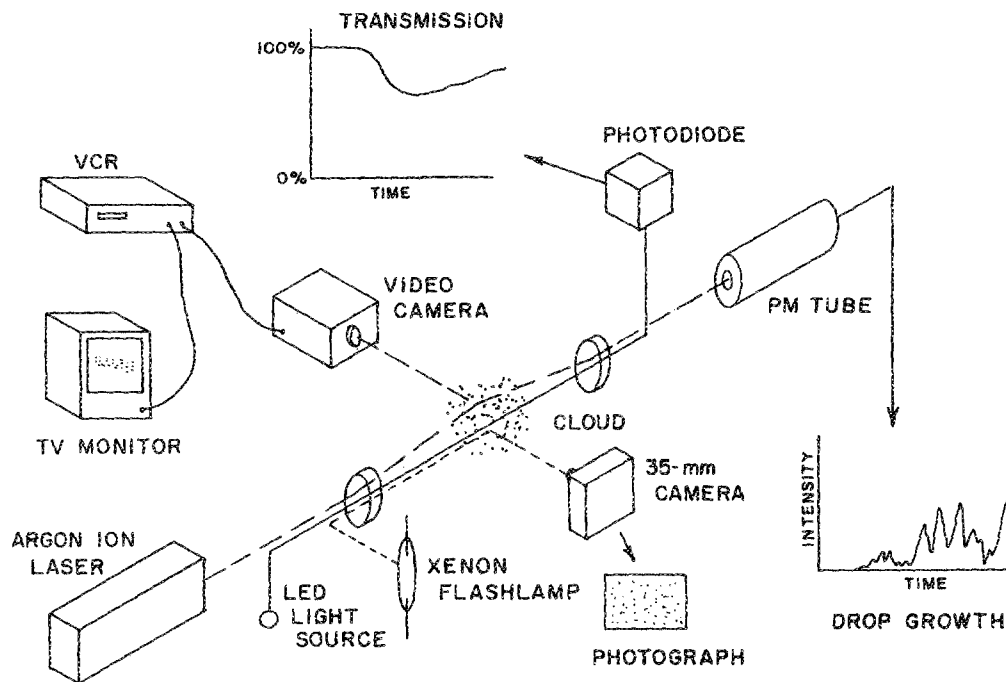


FIG. 6. Schematic view of optical systems.

2. Optical table

The optical diagnostic system for the chamber is mounted on a vibration isolated optical table made of 8-in. iron pipe welded into a horizontal "H" configuration and filled with sand. An argon-ion laser sits on the top of this structure and its expanded beam is directed into the chamber with mirrors mounted on the legs of the "H" which extend around two sides of the chamber.

3. Photographic/video

The cloud in the chamber can be either photographed or viewed with a low-light-level TV camera. Photographs are taken with a motorized Nikon (F3) camera that is computer controlled. An $f/3.5$ Macro Nikkor lens is used with a resolving power of about 150 line pairs/mm (at the film) and a

depth of field of about 1 cm in the center of the chamber. The camera window is at 72° from the forward direction of the laser beam. The film is Kodak Tri-X or Plus-X developed to ISO (ASA) 1600 or 400, respectively, in Diafine developer. Illumination for the photography is provided by a xenon flash lamp powered by a commercial photography electronic flash power supply (200, 400, or 800 J/flash with a 1.4-s, maximum recycle time). The flash lamp light beam is shaped with lenses and a slit into a vertical sheet of light in the chamber. All drops in the light are in focus for the camera lens (in the depth of field) and only these drops are illuminated and register on the film. Calibration of the camera magnification and the illumination volume yields the drop count per cm^3 in the volume (integrated on the film).

A TV camera with a low-light-level silicon tube can be used in place of the photographic camera. The laser beam that is used for Mie scattering measurements provides illumination. Various lenses are available for the camera with views ranging from about 6 cm diameter in the center of the chamber to an extreme wide-angle view obtained by a fisheye lens. This latter arrangement has poor resolution; the other configurations will detect individual cloud drops. The TV camera image may be recorded on a standard VHS video cassette recorder.

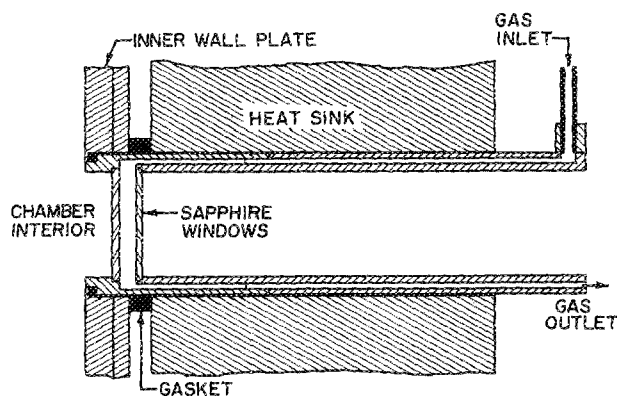


FIG. 7. Observation window design.

4. Optical attenuation

The attenuation system measures the attenuation (or transmission) of a light beam across the chamber. A modified commercial light-emitting diode (LED) provides the light source. The wavelength of approximately 670 nm (20 nm bandwidth) includes few water vapor lines. The small LED source is collimated to a 1-cm beam diameter and projected across the chamber to a silicon diode detector (4° field of view). The intensity-controlled LED source is electroni-

cally chopped at 1 kHz and the detector electronics synchronously rectify this signal. The system is quite immune to background radiation and noise. The light beam is introduced and extracted from the chamber by wavelength selective beam splitters that also transmit the laser beam for Mie scattering. The accuracy of the system is three parts in 10^4 .

5. Mie scattering system

The Mie scattering from a cloud of drops is used to determine the mean size of the drops as a function of time for monodispersed clouds. A 488-nm argon-ion laser beam is introduced into the chamber via a prism at an angle of 2° . A similar prism arrangement on the other side of the chamber views at 2° . Thus the PMT (photomultiplier tube) detector sees the Mie scattering from the cloud drops at 4° from the forward direction. The light scattered from a water sphere (calculated by Mie scattering theory) at 4° is shown in Fig. 8. A similar graph is obtained from the output of the PMT detecting light scattered from a cloud of monodispersed drops growing in time. Comparison of the two graphs (intensity versus radius and intensity versus time) yields radius versus time for the drops in the cloud. One should note in Fig. 8 a very valuable feature of the scattering at 4° . The graph not only displays oscillations of the scattering intensity as a function of radius but reveals that the envelope of the maxima of the oscillations is also modulated. In practice very often the first oscillations in Fig. 8 are difficult to detect due to noise or other factors. The modulation of the envelope allows one to unambiguously correlate a particular oscillation with the correct drop radius.

6. Scanning system

A device to detect, count, and size drops of a polydispersed cloud in a volume of about 1 cm^3 in the center of the chamber is under development. It uses the four strong lines from an argon-ion laser in an integrated and focused beam. The focused spot then is scanned in X , Y , and Z through the

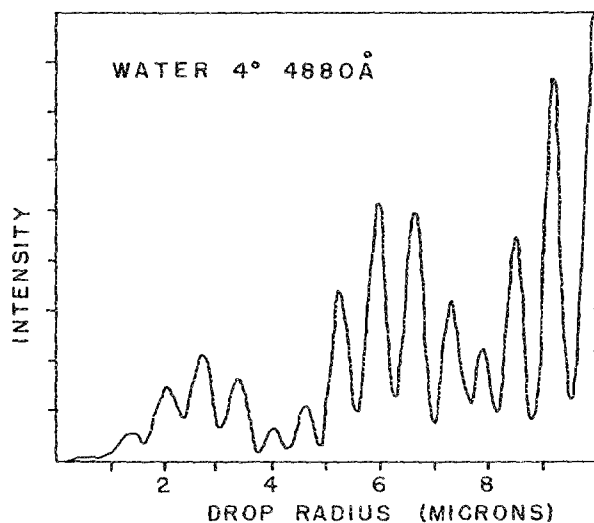


FIG. 8. Four degree Mie scattering intensity vs droplet radius (theoretical calculation).

sample volume. The resulting scattering from the drops is integrated over 15° at 90° from the incoming beam and the height of the pulses are measured. An approximate linear relation has been found theoretically for the height of the pulse as a function of drop size. This system will be mounted at the midpoint of the 122-cm chamber configuration.

II. COMPUTER SYSTEM

A. Proto II

The control and data-acquisition system for the Proto II chamber is built around a NOVA 840 (Data General Corp.) minicomputer (Fig. 9). Two 2.5-Mbyte moving head disk drives with removable cartridges provide on-line storage for both the operating programs and short-term data storage.

A wide-range 15-bit A/D converter with programmable gain and a cycle time of 0.025 s is used for reading temperatures and any routine data acquisition. A high-level 15-bit fixed gain A/D (0–10 V dc) which samples at 10 kHz is used to take measurements requiring a faster acquisition rate (such as the pressure transducer and optical attenuation signals). The high-level A/D can be set to sample at 20 kHz if required.

The digital I/O (input/output) has 12 16-bit channels (seven inputs and five outputs) which are TTL (transistor-transistor logic) compatible. These are used for such functions as reading the external elapsed time clock (10, 100, or 1000 Hz) or outputting on/off commands to the various valves, pumps, recorders, etc. The digital expansion valve command utilizes 8 bits of one output channel. The wall temperature control signal is transmitted through one of the eight D/A analog channels available (five 0–10 V; three ± 10 V).

The operator interacts with the system via both the terminal and the front panel switches on the central processing unit. After an experiment data can be transferred to magnetic tape ($\frac{1}{2}$ -in. reels) for long-term storage or printed on the line printer (Tally T-1120). Both the magnetic tape and line printer are used to store back-up copies of the operating programs.

The computer is capable of multitasking which allows a high degree of flexibility in the chamber operation. By setting up each function such as pressure control, thermometer readings, wall temperature control, etc. as a separate task, it is easy to establish individual priorities and frequencies of performance. Also it is simple to cancel a task entirely for a given experiment. Details are given by Hagen *et al.*⁵

B. Support systems

While the NOVA 840 minicomputer provides control and data-acquisition functions for the simulation facility, a NOVA 3 is used for pre- and post-experiment cloud modeling, experiment preparation, and data analysis. The two minicomputers transfer data by a hardwire link. It is necessary to have a numerical model which simulates the physical processes, e.g., thermodynamics and droplet growth, that occur within the expansion chamber. (This model⁶ runs on the NOVA 3.) The model is used to design and optimize

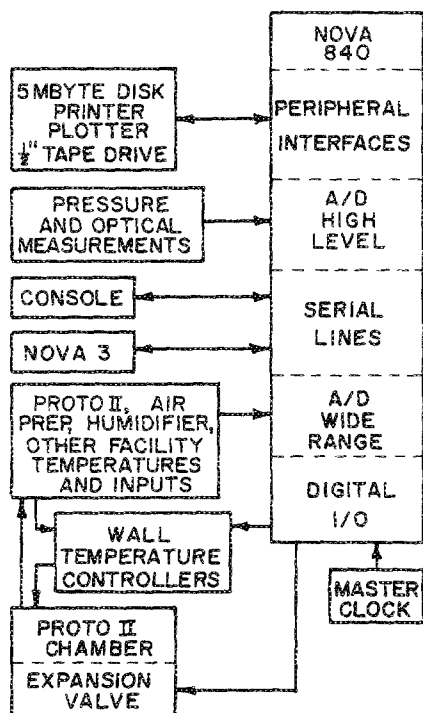


FIG. 9. Block diagram of the computer data-acquisition and control system.

experiments, i.e., choose the best aerosol concentration, expansion profile, data-acquisition times, etc. In the development of a typical experiment, the designer runs the cloud model several times to find variables (initial temperature and pressure, expansion profile, aerosol concentration, etc.) that will yield the conditions desired (e.g., a monodisperse cloud of $4.0\text{-}\mu\text{m}$ radius at 280 K and 90.0 kPa with a growth rate of $0.2\text{ }\mu\text{m/s}$). Computer disk files are generated with this information and then are transferred to the NOVA 840 for real time use in controlling the cloud chamber.

The NOVA 3 also plays a role in the analysis of experiments, i.e., comparing experimental observations such as droplet growth rates with theory under the known conditions. Data files containing results of the experiments are transferred from the NOVA 840 to the NOVA 3 for analysis.

The NOVA 3 also provides computer support for various other cloud simulation facility subsystems. A cold CFD (continuous flow diffusion cloud chamber) with ice on its plates is being developed. The NOVA 3 runs a numerical model that simulates the physical processes (e.g., particle motion, ice nucleation, phoretic forces, ...) that occur in this chamber. It was used for chamber design optimization studies and for data analysis. The aerosol generation and characterization laboratory uses the NOVA 3 to run an inversion program⁷ to process electric mobility classifier aerosol size distribution data. Another program is used to analyze warm (above freezing) CFD aerosol concentration versus supersaturation data to determine the volume soluble fraction spectrum of the aerosol.

III. SAMPLE PREPARATION AND CHAMBER FLUSHING

A. Preparation

Samples for use in the cloud simulation chambers are produced continuously with total volumetric flow rates of $1\text{--}2\text{ l/s}$. Exterior ambient air is drawn in, filtered (particles: 99.97% efficient at $0.3\text{ }\mu\text{m}$; organics: activated carbon), and dried (refrigeration and desiccant: dew point $< -40\text{ }^\circ\text{C}$) to produce clean dry air to which the required water vapor and aerosol concentrations can be added. Water vapor content is established by passing the air through a precision flowing water humidifier. (For dew or frost points below $0\text{ }^\circ\text{C}$ the initial drying process is adjusted to leave the desired vapor content.) The aerosol-laden air is added to the clean moist air using a mixing ratio of $1 : 100$ or less. The resulting sample is then flushed through the appropriate cloud simulation chamber.

B. Humidifier

The vapor density of the sample air for warm cloud experiments is established by means of a precision flowing-water humidifier.⁸ Air is exposed to a flowing water surface under closely controlled thermal conditions and allowed to become nearly saturated at the temperature of the system.

The humidifier consists of two thick wall aluminum cylinders (98 cm high by 16.5 cm i.d.) each containing 60 7-mm-diam glass rods. The cylinders and rods are mounted vertically and water is pumped to the top of the cylinders and allowed to flow down over the surfaces of the glass rods. The air which flows around the rods is never further than 13 mm from a flowing water surface during the 30 s residence time of air in the humidifier.

Temperatures of both the cylinders and flowing water are closely thermostated ($0.010\text{ }^\circ\text{C}$ peak-to-peak fluctuation during a sample flush) by a multiloop feedback control system based on transistor thermometers located in the walls of both cylinders, the water flow, and the outlet air flow. Most of the evaporation and the associated latent heat release occur in the first cylinder, so that the second cylinder acts as a fine adjustment.

Calibration of the humidifier controls, using the simulation chamber as a precision hygrometer, has shown that the actual dew point of the air at $17\text{ }^\circ\text{C}$ is consistently $0.355\text{ }^\circ\text{C}$ below the temperature of the outlet air flow. During normal steady-state operation of the system, the controls force the outlet air to the system set-point temperature and maintain it there with fluctuations of less than $0.010\text{ }^\circ\text{C}$ peak to peak during the period of a sample flush. The error from changes in water-vapor content caused by changes in residence time due to normal variations in the sample air flow rate are smaller than those from other experimental uncertainties.

C. Chamber flushing

A sample is introduced into the chamber using top to bottom flow. It first enters the inlet manifold chamber which is located directly above the simulation chamber top section. The sample then flows into the chamber through 164 sepa-

rate ports. This technique ensures a more uniform flow of sample into the top of the sensitive volume than a single large port. It thus greatly reduces the likelihood of stagnant regions being formed in some corners of the chamber during flushing. An additional very important advantage is that each individual port is small enough to fit in the space between TEM's and does not interfere with their normal physical layout. This inlet system is duplicated as an outlet system on the bottom of the chamber where it is connected to the exhaust line.

The chamber is flushed for a minimum of 15 min. Flushing typically continues until a measurement of the aerosol concentration in the chamber shows an acceptably stable value for 5 min. The sample is drawn from the chamber expansion system which is being flushed with the chamber. When both flushing conditions have been satisfied and all other chamber systems are operating normally, the chamber inlet and outlet valves are closed to seal the chamber.

At this time, pressure control of the chamber by the control computer is activated and a very slow isothermal expansion or compression brings the chamber to the desired initial pressure. A sample line which bypasses the chamber directly to the exhaust line is also opened as the chamber is closed (to allow the steady-state conditions existing in the sample preparation system to be maintained and ready for use in flushing the chamber for the next experiment).

ACKNOWLEDGMENTS

This work has been largely supported by the Office of Naval Research (ONR N00014-75-C-0182; ONR N00014-75-C-0413; ONR N00014-75-C-1152), Air Force Office of Scientific Research (Tri-service funded by ONR, AFOSR, and ARO: AFOSR F49620-80-C-0090; AFOSR 850071), Army Research Office (DAAK 70-C-0241), the National Aeronautics and Space Administration (NASA NAS8-34603; NASA NAS832976; NASA NAS8 31849), and the National Science Foundation (NSFATM 79 19480).

The support and encouragement of J. H. Hughes over the years of development and construction has been greatly appreciated.

¹D. J. Alofs, M. B. Trueblood, D. R. White, and V. L. Behr, *J. Appl. Meteorol.* **18**, 1106 (1979).

²D. J. Alofs, *J. Appl. Meteorol.* **17**, 1286 (1978).

³D. J. Alofs and M. B. Trueblood, *J. Rech. Atmos.* **15**, 219 (1981).

⁴J. L. Schmitt, *Rev. Sci. Instrum.* **52**, 1749 (1981).

⁵D. E. Hagen, K. P. Berkbigler, J. L. Kassner, and D. R. White, in *Mini-computers and Large Scale Computations*, edited by P. Lykos, ACS Symposium Series No. 57 (American Chemical Society, Washington, DC, 1977), pp. 77-93.

⁶D. E. Hagen, *J. Appl. Meteorol.* **18**, 1035 (1979).

⁷D. E. Hagen and D. J. Alofs, *Aerosol Sci. Technol.* **2**, 465 (1983).

⁸D. R. White, A. R. Hopkins, and J. L. Kassner, in *Proceedings of the Moisture and Humidity International Symposium* (Instrument Society of America, Research Triangle Park, NC, 1985).